

Single-photon transport in a waveguide-cavity-emitter system

Xue-Jian Sun

Zhoukou Normal University

Wen-Xiao Liu

North China University of Water Resources and Electric Power

Hao Chen

Qinghai Normal University

Cheng-Yuan Wang

Xi'an Jiaotong University

Hui-Zhong Ma

Zhoukou Normal University

Hong-Rong Li (✉ hrli@mail.xjtu.edu.cn)

Xi'an Jiaotong University

Research Article

Keywords:

Posted Date: May 12th, 2022

DOI: <https://doi.org/10.21203/rs.3.rs-1639989/v1>

License:   This work is licensed under a Creative Commons Attribution 4.0 International License.

[Read Full License](#)

Single-photon transport in a waveguide-cavity-emitter system

Xue-Jian Sun¹, Wen-Xiao Liu², Hao Chen³, Cheng-Yuan

Wang⁴, Hui-Zhong Ma¹ and Hong-Rong Li^{4*}

1. *College of Physics and Telecommunication Engineering,*

Zhoukou Normal University, Zhoukou 466001, China

2. *Department of Physics and Electronics,*

North China University of Water Resources and Electric Power, Zhengzhou, 450046, China

3. *College of Physics and Electronic Information Engineering,*

Qinghai Normal University, Xining 810008, China

4. *Institute of Quantum Optics and Quantum Information,*

School of Physics, Xi'an Jiaotong University, Xi'an 710049, China

Abstract

We investigate the single-photon transport properties in a hybrid waveguide quantum electrodynamics system, in which a one-dimensional waveguide is simultaneously coupled to a cavity and a driven Λ -type three-level atom. The cavity and the atom are also coupled to each other. We show that when the waveguide is coupled to the cavity and the atom at the same point, double electromagnetically induced transparency (EIT) can be observed from the system. The physical mechanism of the double EIT effect has been given by setting up the eigenstate structure for the whole system. When the waveguide is coupled to the cavity and the atom at different points, we demonstrate that the single-photon transmission spectra can be effectively controlled by adjusting the relative separation between the cavity and the atom. Moreover, this non-zero relative separation can lead to the occurrence of the controllable nonreciprocal scattering effect. These results have potential applications in realization of photonic coherent control.

PACS numbers:

*Electronic address: hrli@mail.xjtu.edu.cn

I. INTRODUCTION

Single photons are considered as one of ideal carriers for quantum information, therefore, how to obtain the ability to control and manipulate single photon transport in quantum information processing has been an important issue. Recently, controllable single-photon transport schemes based on the coupling between a one-dimensional (1D) waveguide and emitters, known as waveguide quantum electrodynamics (QED), have been investigated widely both in theory [1-25] and experiment [26-37]. In waveguide QED systems, the emitters serving as quantum nodes, can act as either perfect mirrors reflecting optical fields, or transparency mediums allowing photons to transmit. Many quantum systems can be regarded as the emitters, such as two- or multi-level atoms, quantum dots and cavities containing an atom. The waveguide serves as a quantum channel, which can guide photons to transport along the selected directions. In addition, due to the controllable light-matter interaction, many interesting quantum effects have been revealed in the waveguide QED systems, such as dressed or bound states [38-43], single-photon device [1,2,8-10], many body physics [44,45] and long-range quantum information transfer [46-50].

Compared with various waveguide QED systems, the system combining a cavity QED or a hybrid optomechanics with waveguide has shown more advantages in the aspect of controlling single-photon transport [13,18,22-24]. For example, the nonreciprocal scattering effect have been realized in a 1D waveguide coupled to a cavity QED system [24]. Yang *et al.* investigated the properties of the single-photon routing in a system composed of two waveguides and two coupled cavities interacting with a two-level system. They showed that the single-photon scattering depend strongly on the phase difference between the coupling constants, and the routing properties can be switched on or off by modulating the phase difference [23]. Qiao studied the single-photon transport in a 1D waveguide side coupled to a quadratic optomechanical system. They observed Rabi-splitting-like or an electromagnetically induced transparency (EIT)-like phenomenon from the single-photon transmission spectra [18]. Therefore, studying transport properties in hybrid waveguide QED systems are very interesting and useful.

Motivated by those important works mentioned above, in the present work, we investigate theoretically the single-photon transport in a 1D waveguide coupled to a cavity-EIT system [51], in which a cavity contains a Λ -type three-level atom. As shown in Fig. 1, depending on the available physical realization, the cavity and the three-level atom can couple to this waveguide at one or two different points. Here, we analyze the photon transmission spectra under the two different

cases. Our numerical results show that when the cavity and the atom locate at the same point of the waveguide, an analogous double EIT can be observed from the single-photon spectra. The effects of parameters like the atom-waveguide, the atom-cavity and the cavity-waveguide coupling strengths as well as the detuning between the atom and the cavity on the transmission behavior are studied with more detail; when they locate at different points of the waveguide, the transmission properties can be effectively modified by the relative separation x_0 between the cavity and the three-level atom. Moreover, under this non-zero relative separation condition, the time-reversal symmetry is naturally broken, which leads to a controllable nonreciprocal scattering.

The paper is organized as follows: in section II, we present the theoretical model and derive the transmission amplitude of the single-photon. In section III, the properties of the single-photon transmission are discussed in more detail under the two different conditions $x_0 = 0$ and $x_0 \neq 0$. In section IV, for the case of $x_0 \neq 0$, we demonstrate that the nonreciprocity scattering effect can be achieved. Finally, we conclude our work in section V.

II. MODEL

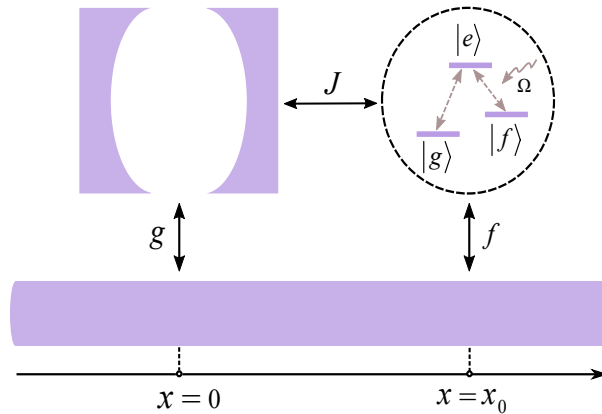


FIG. 1: Schematic configuration of the coupling system. A cavity and a Λ -type three-level atom are coupled to a 1D waveguide at the points $x = 0$ and $x = x_0$ through the coupling strengths g and f , respectively. They are also directly coupled to each other through the coupling strength J .

The system we considered is illustrated in Fig. 1, where a 1D waveguide is coupled to a cavity and a Λ -type three-level atom simultaneously with corresponding coupling strengths g and f . The

cavity and the atom are also coupled to each other through the coupling strength J . The position of the cavity and the emitter are located at $x = 0$ and $x = x_0$, respectively. Note that the cavity and the three-level atom serve as two quantum nodes, which can be equivalently replaced by other quantum setups, such as whispering gallery mode resonators, solid spins, or transmon qubits, etc. As shown in Fig. 1, the atom is characterized by the excited state $|e\rangle$, metastable state $|f\rangle$ and ground state $|g\rangle$. The Hamiltonian of the whole system can be written as $H = H_w + H_{ae} + V$. Here, H_w describes the propagation of the photon in the waveguide, which can be expressed as

$$H_w = \int dx \left\{ -i v_g c_R^\dagger(x) \frac{dc_R(x)}{dx} + i v_g c_L^\dagger(x) \frac{dc_L(x)}{dx} \right\}, \quad (1)$$

where v_g is the group velocity of the photons. $c_R^\dagger(x)$ ($c_R(x)$) and $c_L^\dagger(x)$ ($c_L(x)$) are the bosonic creation (annihilation) operators of the right- and left-going photons at position x , respectively.

The second term H_{ae} denotes the Hamiltonian of the cavity-atom system,

$$H_{ae} = \omega_a a^\dagger a + \omega_e |e\rangle\langle e| + \omega_f |f\rangle\langle f| + \Omega(\sigma_{ef} e^{-i\omega_d t} + \sigma_{fe} e^{i\omega_d t}) + J(a\sigma_{eg} + a^\dagger\sigma_{ge}), \quad (2)$$

where a and a^\dagger are the photon creation and annihilation operators of the single mode cavity with frequency ω_a . $\sigma_{ef} = (\sigma_{fe})^\dagger$ is the transition operator between states $|e\rangle$ and $|f\rangle$. ω_e and ω_f are the frequencies of the states $|e\rangle$ and $|f\rangle$, respectively. The classical control field with strength Ω and frequency ω_d is used to induce the transition between $|e\rangle$ and $|f\rangle$. In the rotating frame, H_{ae} can be written as the time independent form

$$\tilde{H}_{ae} = \omega_a a^\dagger a + \omega_e |e\rangle\langle e| + \delta |f\rangle\langle f| + \Omega(\sigma_{fe} + \sigma_{ef}) + J(a\sigma_{eg} + a^\dagger\sigma_{ge}), \quad (3)$$

with $\delta = \omega_f + \omega_d$.

The third term V in Hamiltonian H represents the waveguide-cavity and the waveguide-atom interactions. The detailed expressions are described as follows:

$$V = g \int dx \delta(x) \{ [c_R^\dagger(x) + c_L^\dagger(x)] a + H.c. \} + f \int dx \delta(x - x_0) \{ [c_R^\dagger(x) + c_L^\dagger(x)] \sigma_{ge} + H.c. \}. \quad (4)$$

In the single-excitation subspace, the eigenstate of the system can be written as

$$|E_k\rangle = \int dx [\phi_R(x) c_R^\dagger(x) + \phi_L(x) c_L^\dagger(x)] |\emptyset, 0_a, g\rangle + \mu_a |\emptyset, 1_a, g\rangle + \mu_e |\emptyset, 0_a, e\rangle + \mu_f |\emptyset, 0_a, f\rangle, \quad (5)$$

where $|\emptyset, m_a, n\rangle$ ($m = 0, 1; n = e, g, f$) represents that the waveguide is in the vacuum state while the cavity and atom are in the states $|m_a\rangle$ and $|n\rangle$, respectively. $\phi_R(x)$ and $\phi_L(x)$ are the single-photon wave function of the right-going and left-going modes in the waveguide. μ_a , μ_e and μ_f

are the excitation amplitudes of the cavity field, the three-level atom in the excited state $|e\rangle$ and metastable state $|f\rangle$, respectively. Solving the stationary Schrödinger equation $H|E_k\rangle = E|E_k\rangle$, the series of coupled equations can be obtained as follows:

$$-i v_g \frac{d\phi_R(x)}{dx} + g\mu_a \delta(x) + f\mu_e \delta(x - x_0) = E\phi_R(x), \quad (6)$$

$$i v_g \frac{d\phi_L(x)}{dx} + g\mu_a \delta(x) + f\mu_e \delta(x - x_0) = E\phi_L(x), \quad (7)$$

$$\omega_e \mu_e + \Omega \mu_f + J \mu_a + f[\phi_R(x_0) + \phi_L(x_0)] = E \mu_e, \quad (8)$$

$$\omega_a \mu_a + J \mu_e + g[\phi_R(0) + \phi_L(0)] = E \mu_e, \quad (9)$$

$$\delta \mu_f + \Omega \mu_e = E \mu_f. \quad (10)$$

We now consider the transport behavior when a single photon with wave vector k is incident from the left side of the waveguide. In this case, the wave functions $\phi_R(x)$ and $\phi_L(x)$ can be written as

$$\phi_R(x) = e^{ikx} \{ \theta(-x) + A[\theta(x) - \theta(x - x_0)] + t\theta(x - x_0) \}, \quad (11)$$

$$\phi_L(x) = e^{-ikx} \{ r\theta(-x) + B[\theta(x) - \theta(x - x_0)] \}, \quad (12)$$

with

$$\theta(x) = \begin{cases} 1 & x > 0 \\ 0 & x = 0. \\ \frac{1}{2} & x < 0 \end{cases} \quad (13)$$

Here, the photon propagates from the regime of $x < 0$, which will experience reflection and transmission when it arrives at the connecting point $x = 0$ and $x = x_0$, respectively. We use r (B) and A (t) to represent the reflection and transmission coefficients of the photon at $x = 0$ ($x = x_0$). $\theta(x)$ shown in Eq. (13) is a step function. Combing Eqs. (6-10) with Eqs. (11-13), we obtain the transmission amplitude t as

$$t = \frac{v_g^2(J^2 - \Delta_e \Delta_a) + 2v_g J g f \sin(kx_0)}{v_g^2(J^2 - \Delta_e \Delta_a) - i v_g (f^2 \Delta_a + g^2 \Delta_e) - 2i f g e^{ikx_0} (f g \sin(kx_0) + J v_g)}, \quad (14)$$

in which $\Delta_e = \Delta - \frac{\Omega^2}{\Delta_f}$, $\Delta = E - \omega_e$, $\Delta_a = E - \omega_a$ and $\Delta_f = E - \delta$. Based on Eq. (14), if we set $\Omega = 0$ and $\omega_e = \omega_a$, the three-level atom is equivalent to a two-level emitter, then we can recover the results given in Ref. [24].

III. SINGLE-PHOTON TRANSMISSION

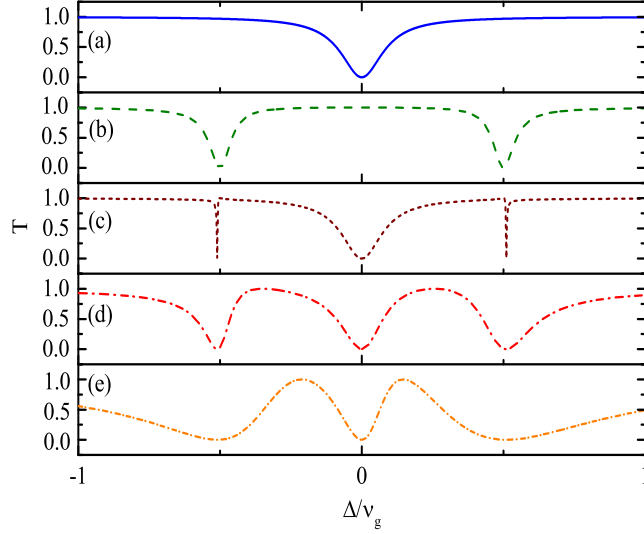


FIG. 2: The transmission rate T as a function of Δ with $\omega_e = \omega_a = \nu_g$, $\delta = 0.5\nu_g$, $\omega_d = 0.5\nu_g$. Other parameters are set as follows: $\{g, f, J, \Omega = 0.3, 0.0, 0.0, 0.0\}\nu_g$, $\{g, f, J, \Omega = 0.0, 0.4, 0.0, 0.5\}\nu_g$, $\{g, f, J, \Omega = 0.3, 0.0, 0.1, 0.5\}\nu_g$, $\{g, f, J, \Omega = 0.3, 0.4, 0.1, 0.5\}\nu_g$ and $\{g, f, J, \Omega = 0.3, 0.8, 0.1, 0.5\}\nu_g$ for (a), (b), (c), (d) and (e), respectively.

In this section, we first study the single-photon transmission properties under the situation of $x_0 = 0$, which means that the waveguide are coupled to the cavity and the atom at the same point. Then, the result shown in Eq. (14) turns out to be

$$t = \frac{\nu_g^2(J^2 - \Delta_e\Delta_a)}{\nu_g^2(J^2 - \Delta_e\Delta_a) - i\nu_g(f^2\Delta_a + g^2\Delta_e) - 2i\nu_g g f J}. \quad (15)$$

The transmission rate $T = |t|^2$ are plotted as a function of the detuning Δ between the incident photon and the atom. This hybrid waveguide QED system can be detached into two kinds of simpler models, that is, the waveguide is only coupled to the cavity or the three-level atom. For the waveguide-cavity coupling case, as shown in Fig. 2(a), when the incident photon is resonant with the cavity, the perfect reflection ($T = 0$) can be induced by the destructive quantum interference between the incoming photon and the reemitted photon by the cavity. Here, we have set $\omega_e = \omega_a$, thus Δ can also represent the detuning between the waveguide and the cavity. The same phenomenon can be observed if the cavity is replaced by a two-level emitter. For the waveguide-atom coupling case, as shown in Fig. 2(b), there is a transparency window located at $\Delta = 0$.

This phenomenon is similar with the traditional EIT. Here, the waveguide serves as a bath for the atom. Under the two-photon resonance condition $\Delta = \Delta_f$, the control field applied to the three-level atom can induce the transition between the states $|f\rangle \leftrightarrow |e\rangle$, leading to two dressed states $|\pm\rangle = \frac{1}{\sqrt{2}}(|e\rangle \pm |f\rangle)$ with energies shifted by $\pm\Omega$, which effectively decay to the same ground state. This would result in a transparency window in the transmission spectra. In Fig. 2(c-e), we investigate more complicate case in which the waveguide is simultaneously coupled to the cavity and the atom at the same point. It's shown that the transmission spectra are characterized by double EIT. Moreover, by tuning the additional coupling strength f between the waveguide and the atom, the position and the width of the two transmission peaks can be effectively adjusted; while, the location of the three absorption dips keep unchanged.

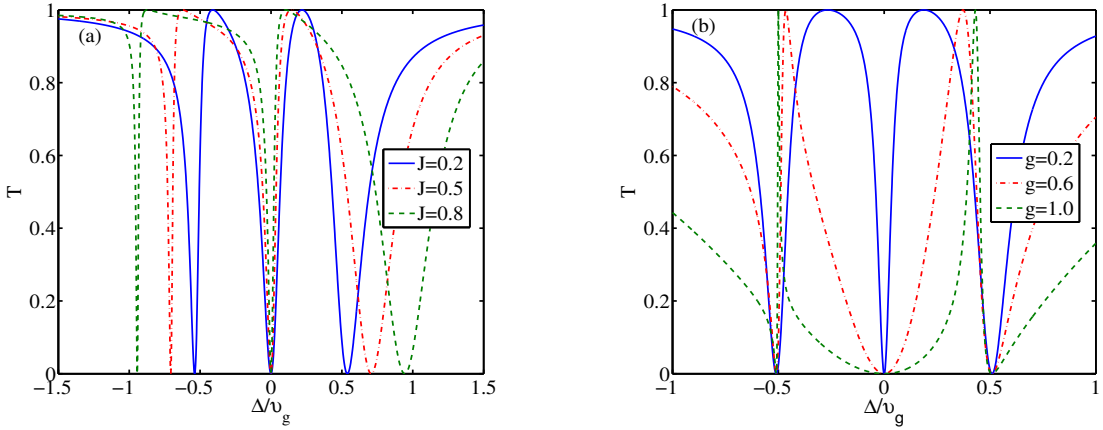


FIG. 3: The transmission rate T as a function of Δ for different (a) the cavity-atom coupling strength J and (b) the waveguide-cavity coupling strength g . Here, we set $\{g, f, \Omega = 0.3, 0.4, 0.5\}v_g$, $\{f, J, \Omega = 0.4, 0.1, 0.5\}v_g$ for (a) and (b), respectively. Other parameters are the same as that in Fig. 2.

Obviously, the cavity-atom and the waveguide-cavity coupling strengths are also important factors affecting the single-photon transmission properties. Figure 3 shows the transmission rate against the detuning Δ with different J and g . It's shown that with increasing of J and g , the symmetry of the transmission spectra can be broken. Moreover, by comparing Fig. 3(a) and Fig. 3(b), we find that except for the absorption dip located at $\Delta = 0$, the position of the other two absorption dips are shifted for different J , but are unchanged for different g . Meanwhile, the two transparency windows shown in Fig. 3(a) and Fig. 3(b) can be effectively adjusted by changing J and g .

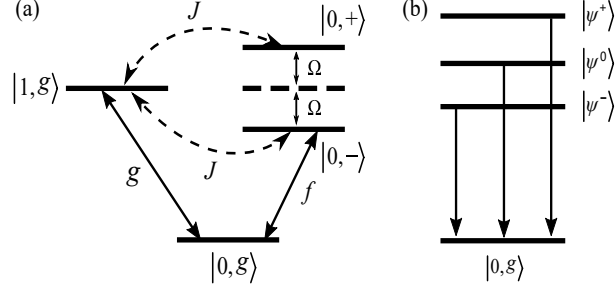


FIG. 4: (a) The energy-level diagram of the cavity-atom system in the single-excitation subspace; (b) the dressed energy structure of the cavity-atom system.

The phenomena mentioned above can be explained by using the energy level diagram of the cavity-atom system shown in Fig. 4. As shown in Fig. 4(a), the photon in waveguide will induce the transition between the states $|0,g\rangle$ and $|1,g\rangle$ or between the states $|0,g\rangle$ and the two dressed states $|0,\pm\rangle$ through the waveguide-cavity or atom coupling, while the transitions between $|1,g\rangle$ and $|0,\pm\rangle$ can be induced by the direct cavity-atom coupling. In this cavity-EIT system, the Hamiltonian \tilde{H}_{ae} can be rewritten in the new basis $\{|1,g\rangle, |0,\pm\rangle\}$, which yields the following three eigenstates

$$\begin{aligned}
 |\psi^\pm\rangle &= \mathfrak{K}^\pm [|1,g\rangle + \frac{J}{\sqrt{2J}(\sqrt{\Omega^2 + J^2} \mp \Omega)} |0,+ \rangle - \frac{J}{\sqrt{2J}(\sqrt{\Omega^2 + J^2} \pm \Omega)} |0,- \rangle], \\
 |\psi^0\rangle &= \mathfrak{K}^0 [|1,g\rangle - \frac{J}{\sqrt{2\Omega}} (|0,+ \rangle + |0,- \rangle)],
 \end{aligned} \tag{16}$$

where $\mathfrak{K}^{0,\pm}$ are the normalization factors. The corresponding eigenvalues are $\omega_\pm = \omega_e \pm \sqrt{J^2 + \Omega^2}$ and $\omega_0 = \omega_e$, respectively. Similar to the cavity EIT system, these eigenstates compose an anharmonic ladder structure as shown in Fig. 4(b). When the incident photon is absorbed into this cavity-atom system, the three transitions from $|0,g\rangle$ to $|\psi^\pm\rangle$ and $|\psi^0\rangle$ can be induced. Then, the absorbed photon will be reemitted through the interaction between the cavity-atom system and the waveguide, and propagates to the left and right sides of the waveguide. Whenever the incident photon is resonant with the three-dressed states in the single-excitation subspace, the destructive interference between directly transmitted photon and this right-going reemitted photons can lead to perfect reflection. According to our theoretical analysis, the complete reflection ($T=0$) should occur at $\Delta = \pm\sqrt{J^2 + \Omega^2}$ and $\Delta = 0$, respectively. This agrees well with our numerical results shown in Fig. 2(c-e) and Fig. 3.

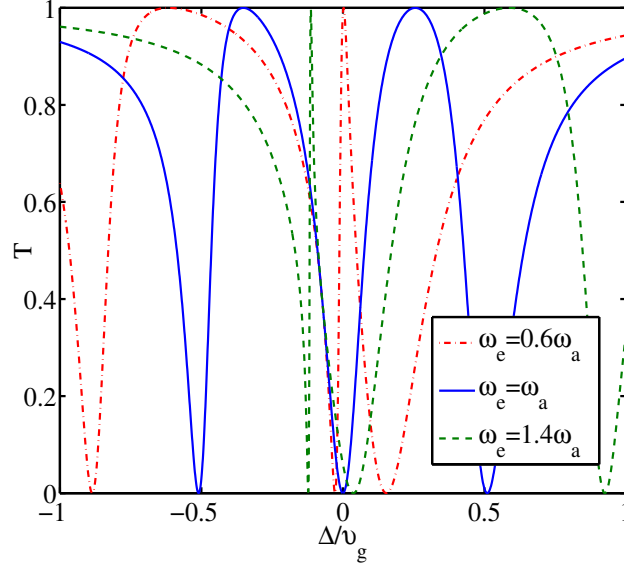


FIG. 5: The transmission rate T as a function of Δ for different detunings between the cavity and the atom. Other parameters are the same as that in Fig. 2.

It's worthy to indicate that the three eigenvalues are obtained under the condition $\omega_e = \omega_a = \delta$ or $\Delta = \Delta_a = \Delta_f$. In general cases, the expression of the eigenvalues depends not only on the cavity-atom coupling strength J and the Rabi frequency of the driving field Ω , but also on the two detunings between the atom and the cavity or the driving field. The effect of the detuning between the cavity and the atom on the transmission rate is explored in Fig. 5. It's clearly shown that for $\omega_e < \omega_a$ ($\omega_e > \omega_a$), the position of the three absorption dips and the two transmission peaks move towards to the negative (positive) direction along the Δ axis. More interestingly, if we tune the cavity-atom detuning from resonance ($\omega_e = \omega_a$) to $0.4v_g$ ($\omega_e = 0.6\omega_a$), the two absorption dips located at $\Delta \sim 0.5 v_g$ and $\Delta = 0$ can convert to two transmission peaks (see the blue solid and the red dot-dashed curves). Thus, the single-photon switch from absorption to transmission can be realized by controlling the cavity-atom detuning. Similar conclusion can be obtained by changing ω_d , therefore, we wouldn't discuss the non-resonant driving case, i.e., $\delta \neq \omega_e$.

In the following parts, we focus on the case $x_0 \neq 0$. For convenience, we still set $\omega_e = \omega_a = \delta$, based on Eq. (14), the complete reflection occurs when

$$E = \omega_e, \quad E_{\pm} = \pm \sqrt{\frac{v_g(J^2 + \Omega^2) + 2gfJ \sin(kx_0)}{v_g}}. \quad (17)$$

Note that the term kx_0 in Eq. (17) functions like the accumulated phase as the travelling photon

moves from one coupling point to the other. The modification of the relative position x_0 on the single-photon transmission is investigated in Fig. 6. As shown in Fig. 6(a), the degree of the transparency denoted by the height of the two peaks become small by changing x_0 . In order to reveal more information about the effect of the relative position on the transmission, we plot T as a function of the detuning Δ and x_0 in Fig. 6(b). As shown in Fig. 6(b), the transmission spectra are characterized by three narrow transmission valleys ($T \simeq 0$) and two transmission peaks between them. Depending on different x_0 , the width of the three absorption valleys can be slightly modulated and the height of the two peaks can be enhanced or suppressed. This position-dependent effect can be explained based on Eq. (17), in which E_{\pm} is not exactly equal to the corresponding dressed state energy ω_{\pm} of the Hamiltonian \tilde{H}_{ae} . As shown in Eq. (17), E_{\pm} has been slightly modulated by x_0 . As a result, the photon transmission shows a phase modulation in the terms of x_0 .

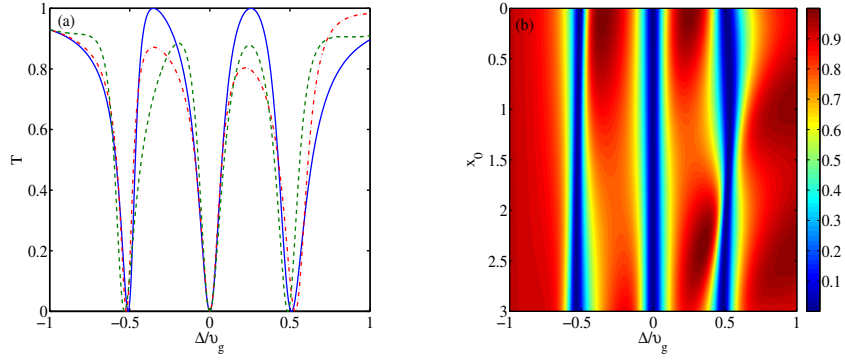


FIG. 6: (a) The transmission rate T as a function of Δ for different x_0 . The blue solid, red dot-dashed and olive dashed curves correspond to $x_0 = 0$, $x_0 = 1$ and $x_0 = 2$, respectively; (b) The transmission rate T as a function of E and x_0 . The parameters are set as $\{g, f, J, \Omega = 0.3, 0.4, 0.1, 0.5\}v_g$. Other parameters are the same as that in Fig. 2.

IV. NONRECIPROCAL BEHAVIOR OF THE SYSTEM

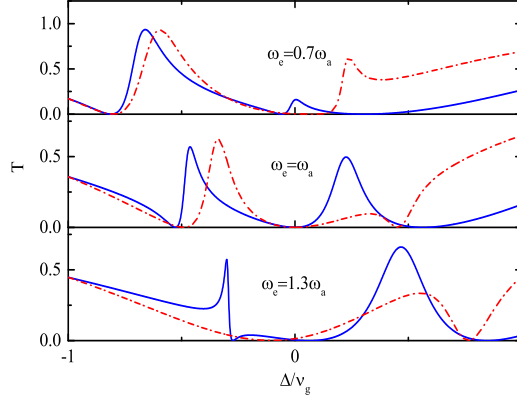


FIG. 7: The transmission rate $T^{L\rightarrow R}$ and $T^{R\rightarrow L}$ as a function of Δ/v_g for different ω_e . Here, we set $\{g, f, J, \Omega = 0.8, 0.8, 0.1, 0.5\}v_g$ and $x_0 = 0.3$. Other parameters are the same as that in Fig. 2. The blue solid and red dot-dashed curves represent the transmission rates $T^{L\rightarrow R}$ and $T^{R\rightarrow L}$, respectively.

Due to the potential applications in quantum information processing, the nonreciprocal transmission has been widely studied in waveguide QED systems. For example, Ref. [24] reported that when a 1D waveguide is coupled to a two-level emitter-cavity interacting system, by controlling the phase difference between the emitter and the cavity, the nonreciprocal phenomenon can be realized. It's natural to ask when we use a Λ -type three-level emitter instead of the two-level emitter in the above system and ignore the effect of the phase difference on the transmission spectra, whether such kind of nonreciprocal behavior can still be obtained. In order to answer this question, we plot the single photon transmission rate $T^{L\rightarrow R}$ and $T^{R\rightarrow L}$ as a function of E/v_g in Fig. 7. Here, $T^{L\rightarrow R}$ ($T^{R\rightarrow L}$) describes the transmission rate when the incident photons propagate from left (right) to right (left). The transmission rate $T^{R\rightarrow L}$ can be calculated by defining a new transmission amplitude t' . The expression of t' can be obtained by changing x_0 in Eq. (14) to $-x_0$, which gives

$$t' = \frac{v_g^2(J^2 - \Delta_e\Delta_a) - 2v_gJgf \sin(kx_0)}{v_g^2(J^2 - \Delta_e\Delta_a) - iv_g(f^2\Delta_a + g^2\Delta_e) + 2ifge^{-ikx_0}(fg \sin(kx_0) - Jv_g)}. \quad (18)$$

Figure 7 clearly shows that for both resonant and non-resonant cases, $T^{L\rightarrow R}$ can be larger or smaller than $T^{R\rightarrow L}$ depending on different incident photon frequency.

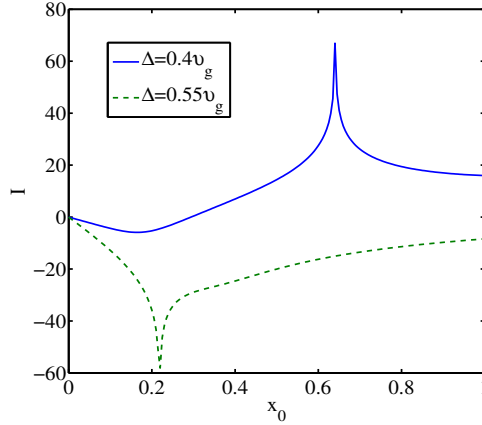


FIG. 8: The isolation rate I as a function of x_0 for different Δ . Here, we consider the resonance case $\omega_e = \omega_a = \delta = v_g$. Other parameters are the same as that in Fig. 7.

In addition, as we mentioned above, the transmission rate can be affected by the relative distance x_0 . Therefore, the nonreciprocal scattering effect can also be controlled by adjusting x_0 . In order to clearly present how the incident photon frequency and x_0 affect the nonreciprocal behavior of the system, we define the isolation ratio I as

$$I(\text{dB}) = -10 \log_{10} \frac{T^{\text{R} \rightarrow \text{L}}}{T^{\text{L} \rightarrow \text{R}}}, \quad (19)$$

which is plotted as a function of x_0 in Fig. 8. It's shown that when $\Delta = 0.4v_g$ and $\Delta = 0.55v_g$, the absolute values of isolation ratio can reach as high as $|I| = 67$ dB and $|I| = 58$ dB at $x_0 \simeq 0.64$ and $x_0 \simeq 0.22$, respectively. Therefore, a controllable single-photon nonreciprocal transmission can be achieved in our system. The physical reason behind the single-photon nonreciprocal transmission is that when we rewrite the Hamiltonian in the momentum space and change i to $-i$, the expression of the Hamiltonian cannot keep the original form. In other words, when the cavity and the emitter is located at different points of the waveguide, the time-reversal symmetry cannot maintain, which leads to the single-photon nonreciprocal transmission. It's worthy to point out that only when the coupling strength g and f are strong, the nonreciprocal effect is obvious. This is different from the two-level emitter case as shown in Ref. [24], in which the nonreciprocal scattering behavior is strong even g and f are weak.

V. CONCLUSION

In conclusion, we investigated the single-photon scattering in a 1D waveguide which is simultaneously coupled to a single cavity and a driven Λ -type three-level atom. The atom acts as a quantum node and is directly coupled to the cavity as well. We showed that when the waveguide is coupled to the cavity-atom system at the same point, the double EIT phenomenon can be observed from the single-photon transmission spectra. In order to give an explicit explanation of the double EIT, we set up the eigenstate structure for the system. Moreover, the effects of the waveguide-cavity or atom, the cavity-emitter coupling strengths, and the detuning between the cavity and the atom on the single photon properties are discussed in more detail. When the waveguide is coupled to the cavity and the atom at different points, we demonstrate that the properties of the single-photon transmission present position-modulated effect. In particular, we have shown that the controllable nonreciprocal scattering can be realized by adjusting the incident photon frequency and the relative separation x_0 between the cavity and the atom. These results can be applied to realize photonic coherent control in waveguide systems.

-
- [1] Shen, J.T and Fan, S.H, Coherent photon transport from spontaneous emission in one-dimensional waveguides, *Opt. Lett.* (30), 2001 (2005).
 - [2] Zhou, L and Gong, Z. R and Liu, Yu-xi and Sun, C P and Nori, F, Controllable scattering of a single photon inside a one-dimensional resonator waveguide, *Phys. Rev. Lett.*(101), 100501 (2008).
 - [3] Shen, J.T and Fan, S.H, Theory of single-photon transport in a single-mode waveguide. I. Coupling to a cavity containing a two-level atom, *Phys. Rev. A*(79), 023837(2009).
 - [4] Shen, J.T and Fan, S.H, Theory of single-photon transport in a single-mode waveguide. II. Coupling to a whispering-gallery resonator containing a two-level atom, *Phys. Rev. A* (79), 023838 (2009).
 - [5] Tsoi, T.S and Law, C.K, Single-photon scattering on Λ -type three-level atoms in a one-dimensional waveguide, *Phys. Rev. A* (80), 033823 (2009).
 - [6] Witthaut, D and Sørensen, A.S, Photon scattering by a three-level emitter in a one-dimensional waveguide, *New. J. Phys.* (12), 043052 (2010).
 - [7] Jia, W.Z and Wang, Z.D, Single-photon transport in a one-dimensional waveguide coupling to a hybrid atom-optomechanical system, *Phys. Rev. A* (88), 063821 (2013).

- [8] Neumeier, L and Leib, M and Hartmann, M.J, Single-photon transistor in circuit quantum electrodynamics, *Phys. Rev. Lett.* (111), 063601 (2013).
- [9] Huang, J.F and Shi, T and Sun, C.P and Nori, F, Controlling single-photon transport in waveguides with finite cross section, *Phys. Rev. A* (88), 013836 (2013).
- [10] Qin, W and Nori, F, Controllable single-photon transport between remote coupled-cavity arrays, *Phys. Rev. A*(93), 032337 (2016).
- [11] Liao, Z.Y and Nha, H and Zubairy, M.S, Dynamical theory of single-photon transport in a one-dimensional waveguide coupled to identical and nonidentical emitters, *Phys. Rev. A*(94), 053842 (2016).
- [12] Liao, Z.Y, Zeng, X.D, Nha, H and Zubairy, M.S, Photon transport in a one-dimensional nanophotonic waveguide QED system, *Phys. Scr.*(91), 063004 (2016).
- [13] Cheng, M.T and Ma, X.S and Zhang, J.Y and Wang, B, Single photon transport in two waveguides chirally coupled by a quantum emitter, *Opt. Exp.* (24), 19988 (2016).
- [14] Yu, X.Y and Li, J.H, Coherent manipulation of singlephoton propagation in a one-dimensional waveguide with multiple Λ -type periodically arrayed atoms, *J. Opt. Soc. Am. B* (33),165 (2016).
- [15] Roy, D, Wilson, C.M and Firstenberg, O, Colloquium: Strongly interacting photons in one-dimensional continuum, *Rev. Mod. Phys.* (89), 021001 (2017).
- [16] Cheng, M.T, Xu, J.P and Agarwal, G.S, Waveguide transport mediated by strong coupling with atoms, *Phys. Rev. A* (95), 053807 (2017).
- [17] Konyk, W and Gea-Banacloche, J, One-and two-photon scattering by two atoms in a waveguide, *Phys. Rev. A* (96), 063826 (2017).
- [18] Qiao, L, Single-photon transport through a waveguide coupling to a quadratic optomechanical system, *Phys. Rev. A*(96), 013860 (2017).
- [19] Das, S and Elfving, V.E, Reiter, F and Sørensen, A.S, Photon scattering from a system of multilevel quantum emitters. I. Formalism, *Phys. Rev. A* (97), 043837 (2018).
- [20] Das, S, Elfving, V E, Reiter, F and Sørensen, A.S, Photon scattering from a system of multilevel quantum emitters. II. Application to emitters coupled to a one-dimensional waveguide, *Phys. Rev. A* (97), 043838 (2018).
- [21] Yan W B, Ni W Y, Zhang J, Zhang F Y and Fan H. Tunable single-photon diode by chiral quantum physics. *Phys. Rev. A* (98), 043852 (2018).
- [22] Zhang, Y.Q, Zhu, Z.H, Peng, Z.H, Jiang, C.L, Chai, Y.F, Hai, L and Tan, L, Controlling single-photon

- transport in an optical waveguide coupled to an optomechanical cavity with a Λ -type three-level atom, *Laser Phys. Lett.* (15), 065209 (2018).
- [23] Yang D.C, Cheng M.T, Ma X.S, Xu J, Zhu C, Huang X.S. Phase-modulated single-photon router. *Phys. Rev. A*(98), 063809 (2018).
- [24] Wang, Z, Du, L, Li, Y and Liu, Y.X. Phase-controlled single-photon nonreciprocal transmission in a one-dimensional waveguide. *Phys. Rev. A* (100), 053809 (2019).
- [25] Debsuvra, M, Girish, S.A, Transparency in a chain of disparate quantum emitters strongly coupled to a waveguide, *Phys. Rev. A* (101), 063814 (2020).
- [26] Akimov, A.V, Mukherjee, A, Yu, C.L , Chang, D.E, Zibrov, A.S, Hemmer, P.R, Park, H and Lukin, M.D, Generation of single optical plasmons in metallic nanowires coupled to quantum dots, *Nature* (London). (450), 402 (2007).
- [27] Dayan, B, Parkins, A.S, Aoki, T, Ostby, E.P, Vahala, K.J and Kimble, H.J, A photon turnstile dynamically regulated by one atom, *Science* (319), 5866 (2008).
- [28] Wei, H, Ratchford, D, Li, X, Xu, H, and Shih, C.K, Propagating surface plasmon induced photon emission from quantum dots, *Nano Lett.* 9, 4168 (2009).
- [29] Huck, A, Kumar, Shakoor, S.A, and Andersen, U.L, Controlled Coupling of a Single Nitrogen-Vacancy Center to a Silver Nanowire, *Phys. Rev. Lett.* (106), 096801 (2011).
- [30] Babinec, T. M, Hausmann, B. J. M, Khan, M, Zhang, Y, Maze, J. R, Hemmer, P. R, and Loncar, M, A diamond nanowire single-photon source, *Nat. Nanotechnol.* 5, 195 (2010).
- [31] Claudon, J, Bleuse, J, Malik, N. S, Bazin, M, Jaffrennou, P, Gregersen, N, Sauvan. C, Lalanne, P, and Gérard, J.M, A highly efficient single-photon source based on a quantum dot in a photonic nanowire, *Nat. Photonics* (4), 174 (2010).
- [32] Astafiev, O, Zagoskin, A.M, Abdumalikov, A.A, Pashkin, YU.A, Yamamoto, T, Inomata, K, Nakamura, Y, and Tsai, J.S, Resonance fluorescence of a single artificial atom, *Science* (327), 840 (2010).
- [33] Hoi, I.C, Wilson, C.M, Johansson, G, Palomaki, T, Peropadre, B, and Delsing, P, Demonstration of a Single-Photon Router in the Microwave Regime, *Phys. Rev. Lett.* (107), 073601 (2011).
- [34] Yalla, R, Sadgrove, M, Nayak, K.P, and Hakuta, K, Cavity Quantum Electrodynamics on a Nanofiber Using a Composite Photonic Crystal Cavity, *Phys. Rev. Lett.* 113, 143601 (2014).
- [35] Javadi, A, Söllner, I, Arcari, M, Lindskov Hansen, S, Midolo, L, Mahmoodian, S, Kiršanské, G, Pregolato, T, Lee, E. H, Song, J.D, Stobbe, S, and Lodahl, P, Single-photon non-linear optics with a

- quantum dot in a waveguide, *Nat. Commun.* 6, 8655 (2015).
- [36] Goban, A, Hung, C.L, Hood, J.D, Yu, S.P, Muniz, J. A, Painter, O, and Kimble, H.J, Superradiance for Atoms Trapped Along a Photonic Crystal Waveguide, *Phys. Rev. Lett.* 115, 063601 (2015).
- [37] Sipahigil, Alp and Evans, Ruffin E and Sukachev, Denis D and Burek, Michael J and Borregaard, Johannes and Bhaskar, Mihir K and Nguyen, Christian T and Pacheco, Jose L and Atikian, Haig A and Meuwly, Charles, An integrated diamond nanophotonics platform for quantum-optical networks, *Science.* (354), 847 (2016).
- [38] Zheng, H, Gauthier, D.J and Baranger, H.U, Many-body bound-state effects in coherent and Fock-state scattering from a two-level system, *Phys. Rev. A* 82, 063816 (2010).
- [39] Shi, T, Wu, Y.H, González-Tudela, A and Cirac, J.I, Bound states in boson impurity models, *Phys. Rev. X* 6, 021027 (2016).
- [40] Calajó, G, Ciccarello, F, Chang, D.E and Rabl, P, Atom-field dressed states in slow-light waveguide QED, *Phys. Rev. A* 93, 033833 (2016).
- [41] Sánchez-Burillo, E, Zueco, D, Martín-Moreno, L and García-Ripoll, J.J, Dynamical signatures of bound states in waveguide QED, *Phys. Rev. A* 96, 023831 (2017).
- [42] Fong, P.T and Law, C.K, Bound state in the continuum by spatially separated ensembles of atoms in a coupled-cavity array, *Phys. Rev. A* 96, 023842 (2017).
- [43] Calajó, G, Fang, Y.L.L, Baranger, H.U and Ciccarello, F, Exciting a bound state in the continuum through multiphoton scattering plus delayed quantum feedback, *Phys. Rev. Lett.* 122, 073601 (2019).
- [44] Douglas, J.S, Habibian, H, Hung, C.L, Gorshkov, A.V, Kimble, H.J, and Chang, D. E, Quantum many-body models with cold atoms coupled to photonic crystals, *Nat. Photon.* 9, 326 (2015).
- [45] Richerme, P, Gong, Z.X, Lee, A, Senko, C, Smith, J, Floss-Feig, M, Michalakis, S, Gorshkov, A. V, and Monroe, C, Non-local propagation of correlations in quantum systems with long-range interactions, *Nature* (511), 198 (2014).
- [46] Zheng, H.X and Baranger, Harold U, Persistent quantum beats and long-distance entanglement from waveguide-mediated interactions, *Phys. Rev. Lett.* (110), 113601 (2013).
- [47] Gonzalez-Ballesteros, C, Gonzalez-Tudela, A, Garcia-Vidal, F.J and Moreno, E, Chiral route to spontaneous entanglement generation, *Phys. Rev. A* (92), 155304 (2015)
- [48] Mok, W.K, You, J.B, Kwek, L.C and Aghamalyan, D, Microresonators enhancing long-distance dynamical entanglement generation in chiral quantum networks, *Phys. Rev. A* (101), 053861 (2020).
- [49] Yu, Y, Ma, F, Luo, X.Y, Jing, B, Sun, P.F, Fang, R.Z, Yang, C.W, Liu, H, Zheng, M.Y, Xie, X.P, Zhang,

- W.J, You, L.X, Wang, Z, Chen. T.Y, Zhang. Q, Bao. X.H, and Pan. J.W, Entanglement of two quantum memories via fibres over dozens of kilometres, *Nature* 578, 240 (2020).
- [50] Leent, T, Bock, M, Garthoffff, R, Redeker, K, Zhang, W, Bauer, T, Rosenfeld, W, Becher, C, and Weinfurter, H, Long-distance distribution of emitter-photon entanglement at telecom wavelength, *Phys. Rev. Lett.* 124, 010510 (2020).
- [51] Souza, J. A and Villas, C.J, Coherent control of quantum fluctuations using cavity electromagnetically induced transparency, *Phys. Rev. Lett.* 111, 113602 (2013).